Laboratori Nazionali di Frascati

To be submitted to Nuclear Instr. & Meth.

LNF-88/06(P)
3 Febbraio 1988

R.Boni, V.Chimenti, B.Spataro, F.Tazzioli, P.Fernandes and R.Parodi:

DESIGN AND OPERATION OF A MULTIPACTING-FREE 51.4 MHz RF ACCELERATING CAVITY

Servizio Documentazione
dei Laboratori Nazionali di Frascati
P.O. Box, 13 - 00044 Frascati (Italy)

INFN - Laboratori Nazionale di Frascati
Servizio Documentazione

LNF-88/06(P)
3 Febbraio 1988

DESIGN AND OPERATION OF A MULTIPACTING-FREE 51.4 MHz RF ACCELERATING CAVITY

R.Boni, V.Chimenti, B.Spataro, F.Tazzioli
INFN - Laboratori Nazionali di Frascati, P.O. Box 13, 00044 Frascati (Italy)

P.Fernandes
Istituto di Matematica Applicata del CNR - Genova (Italy)

R.Parodi
INFN - Sezione di Genova (Italy)

Abstract

The operation of the Frascati storage ring RF accelerating cavity, whose design voltage range was intended to be from a few kV to 200 kV, was affected by resonant discharges in the 30-80 kV range . Computer simulations clearly showed high level multipacting discharges located on the end-plates of the resonator. A cavity model was built for investigating appropriate solutions. The design and the construction of a multipacting-free resonator of new shape, was successfully carried out. The experimental results are presented in this paper.

Introduction

The accelerating RF cavity of the Frascati 1.5 GeV electron storage ring Adone consists of a reentrant single cell resonator working at 51.4 MHz, the 18th harmonic of the particle revolution frequency. The cavity is made of aluminium and is in ultra-vacuum. In Table I is presented a set of the main parameters of the resonator and Fig. 1 shows a quadrant of the longitudinal section of the cavity evidencing the flux lines of the accelerating electric field.

TABLE I

Resonant frequency	Fo = 51.410 MHz
Accelerating voltage	Va = 200 kV
Unloaded quality factor	Qo = 16,000
Shunt-impedance	Zsh = 3 Mohm
Dissipated power	Pd = 13 kW

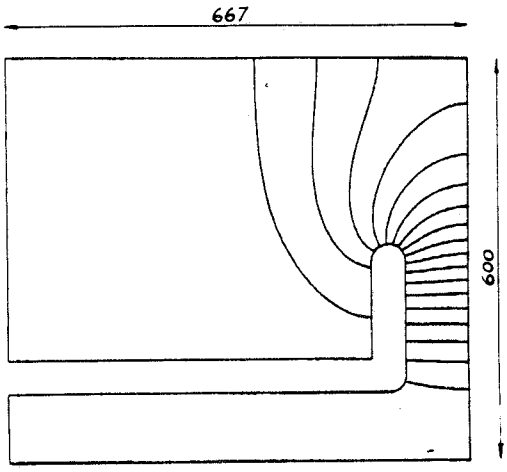

FIG.1 - Longitudinal section of the cavity with the flux lines of the accelerating electric field.

The behaviour of the cavity resonator was strongly affected by resonant discharges (multipacting)[1,2,3]. This is a well known phenomenon in evacuated RF cavities, which leads to a resonant multiplication of the electrons emitted by the walls, accelerated and deflected by the electromagnetic fields ; the particles oscillate between the same or two points of the resonator inner surface extracting other particles at each impact if particular conditions like the energy of the collisions, the level and phase of the fields, are fulfilled.

The operation of the Adone cavity was inhibited by multipacting (m.p.) for a range of the accelerating voltage between 30 and 80 kV. High peak power RF pulses with steep rise time were therefore required from the feeding amplifier to overcome the barrier, the peak power being much greater than that needed for regime operation. This caused serious problems to the RF equipments[4]. Besides this, one had to be very careful not to let air into the cavity, because the surface oxidation enhanced the secondary emission coefficient and a long conditioning by RF pulsing was necessary to set the cavity again in operation. A sample of the RF fields was detected through a small loop located into the cavity. The m.p. level was evidenced by the sharp variation of the slope of the exponential decay at about 70 kV as shown in Fig. 2.

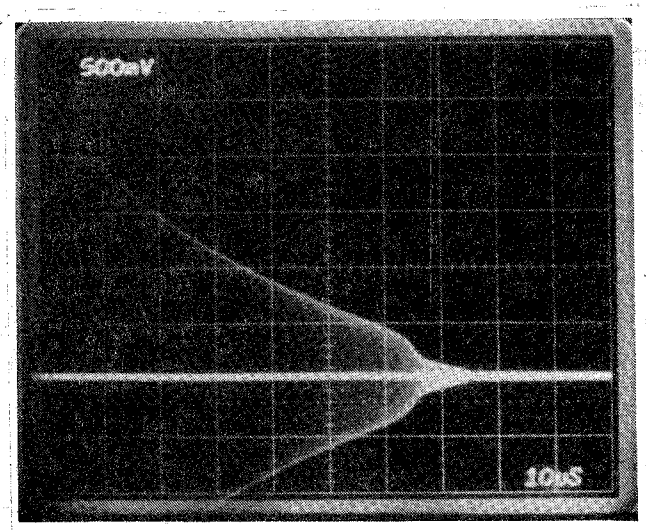

FIG. 2 - Tail of an RF pulse evidencing the m.p. level. (v = 100 kV/cm).

Investigations by a simulator code

The use of the computer code Newtraj (see Appendix A) which simulates the resonant discharge phenomena in resonators under vacuum, allowed us to investigate the behaviour of the Adone accelerating cavity and to compare the calculated and the experimental data.

The "Newtraj" code solves the motion equations of a charged particle in the RF fields of the cavity under study. The values of the EM fields for the device of interest are taken from OSCAR2D code[5,6]. The particle is followed through its path inside the cavity and the probability of the production of back-scattered particles is calculated after each impact with the inner surface.

A resonant discharge is characterized by multiple, nearly overlapping, paths and by an increasing production rate of re-emitted particles.

Many code simulations of possible m.p. discharges were made for the Adone cavity. The range of accelerating voltage from 30 to 150 kV was carefully investigated. According to the measurements made on the cavity, the Newtraj program found strong resonant discharges between 30 and 70 kV. Fig. 3 presents a plot of a resonant trajectory for an accelerating voltage of 50 kV. For this case a very high production rate of secondary particles is evidenced by the computer program. The plot shows that the trajectories tend to be concentrated in the flat end-plates region where the weak electric RF field and the intense magnetic RF field force the particles to follow closed paths.

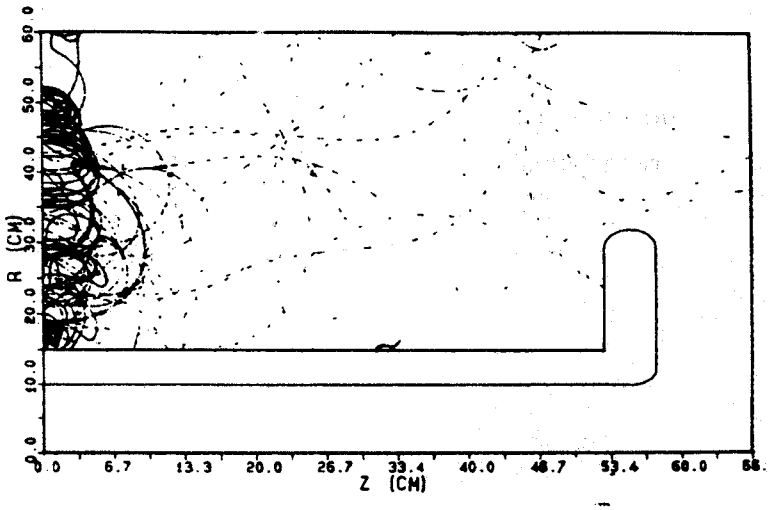

FIG. 3 - Resonant trajectory for V = 50 kV.

The cavity model

In order to check the validity of the results given by the Newtraj code, we decided to build a small cavity model that would allow experiments with moderate power. A picture of the model is shown in Fig. 4.

The RF parameters were :

- resonant frequency F_o = 99.500 MHz
- unloaded quality factor Q_o = 6,500
- shunt-impedance R_{sh}= 0.8 MΩ.

With a 300 W RF generator we were able to reach 15 kV at the gap. Before evacuating, the cavity internal surface was simply cleaned with abrasive powder and demineralized water, without organic solvents. Vacuum tightness was ensured by Viton gaskets and moderate baking was made to reach a basic pressure of about $3x10^{-8}$mbar in the absence of RF.

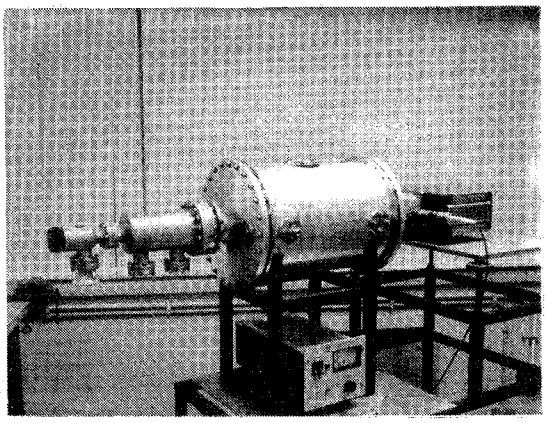

FIG. 4 - The cavity model under test.

Besides the feeding and pick-up loops, a small probe was mounted on an end-plate for detecting the electron current caused by the discharge. In Fig. 5 is shown a photo of an RF pulse in presence of m.p. level at about 2.5 kV at the cavity gap. In coincidence with the m.p. discharge an electron current is detected by the probe. See the negative step in the upper trace of Fig. 5.

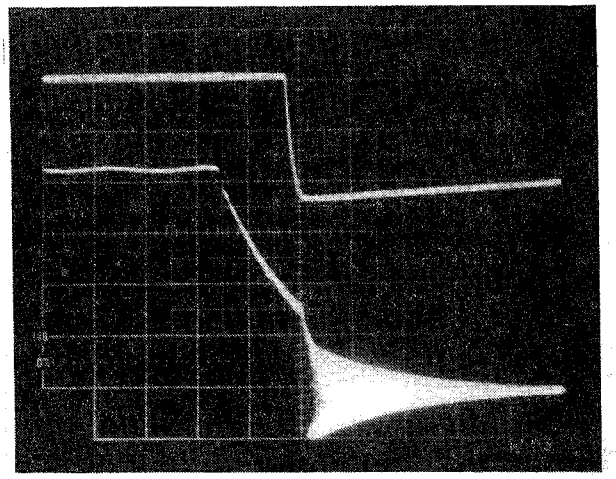

FIG. 5 - Resonant discharge for the model at 2.5 kV (50μsec/cm). Upper trace: integrated current from the probe in coincidence with the m.p. discharge. Lower trace: gap voltage.

The computer simulations executed with "Newtraj" indicate that these discharges took place between the inner electrodes and the outer envelope of the cavity as showed in Fig. 6.

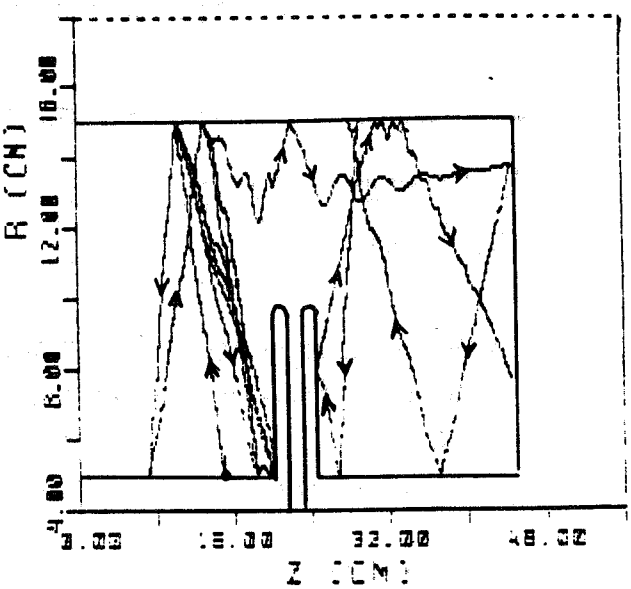

FIG. 6 - Resonant trajectory for the model at 2.5 kV.

Therefore, a very thin layer of graphite powder mixed with silicone resin used as a binder, was applied on those regions for decreasing the secondary emission of the surface.

The results of this procedure was that the previous m.p. level disappeared and no current was detected by the probe. This confirmed the localization of the discharges made by Newtraj and convinced us to intervene on the 51.4 MHz Adone cavity according with the indications of the program.

Cure of the Adone accelerating cavity

The results of the investigations made on the model with the aid of Newtraj-code, induced us to use the same procedure for the storage ring resonator. Different treatments, like sputtering of titanium on the zones of the inner surface responsible of m.p., were not successfull because the available apparatus (Ti-ball) did not allow a good deposition process.

The results with graphite were instead fully satisfactory. RF power was fed again into the cavity without the need of conditioning. The high level m.p. thresholds vanished. Only the m.p. between the capacitive plates was still detected but, because of its low level (~4-5 kV), it did not affect the operation of the resonator which became fully reliable.

Multipacting simulations and design of a resonator of new shape

The solution illustrated above was only temporary because the graphite layer is not well suited for ultra-high vacuum. A new cavity resonator was therefore designed. Starting from the consideration that a spherically shaped cavity is free of electron m.p.[7,8], we applied this principle[9] to the shape of the end-plates of our resonator giving them a rounded form as shown in Fig.7.

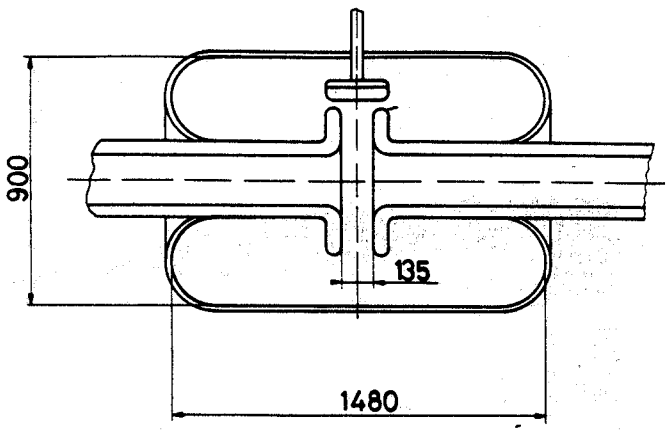

FIG. 7 - The new shaped cavity resonator.

Due to this shape, a strong radial component Er of the surface electric field is everywhere present along the rounded end-plate. This Er component inverts its sign at the midpoint of the arc. Therefore a secondary electron, emitted from a point of the surface of the end-plate, is sweept away from the impact region toward the midpoint of the arc where it stops because the kinematical

conditions for the resonant discharge are no more fulfilled. Near the mid-point, in fact, the surface electric field is so small that the energy gain of the secondary electron is not enough to produce a relevant electron multiplication.

In Fig. 8 is presented a plot of a trajectory near the rounded end-plate for a gap voltage of 60 kV. The secondary electron shown in the figure stops after a small number of impacts.

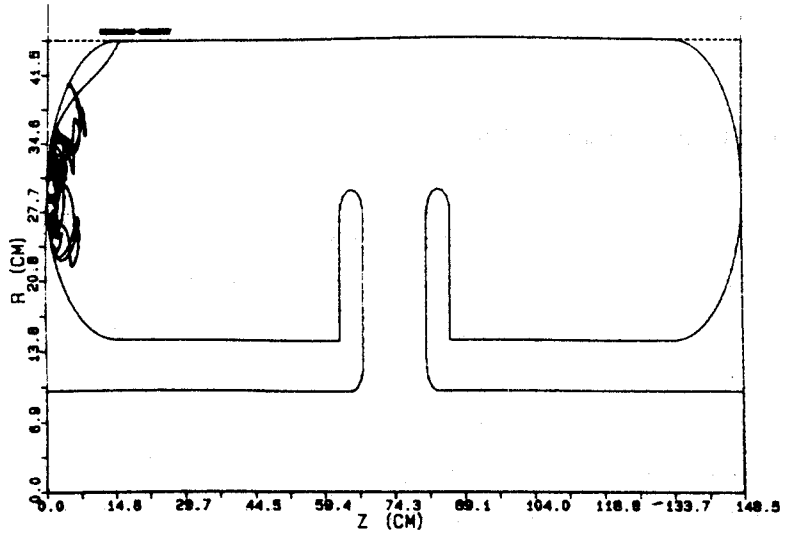

FIG. 8 - Non resonant trajectory for the new cavity (not to scale) at 60 kV.

Experimental results

The new cavity resonator has been successfully tested. Fig. 9 shows a picture of the cavity.

In accord with the computer simulations, the new resonator presents no high voltage discharges but only a very soft m.p. threshold at 12 kV gap voltage (see Fig.10) .

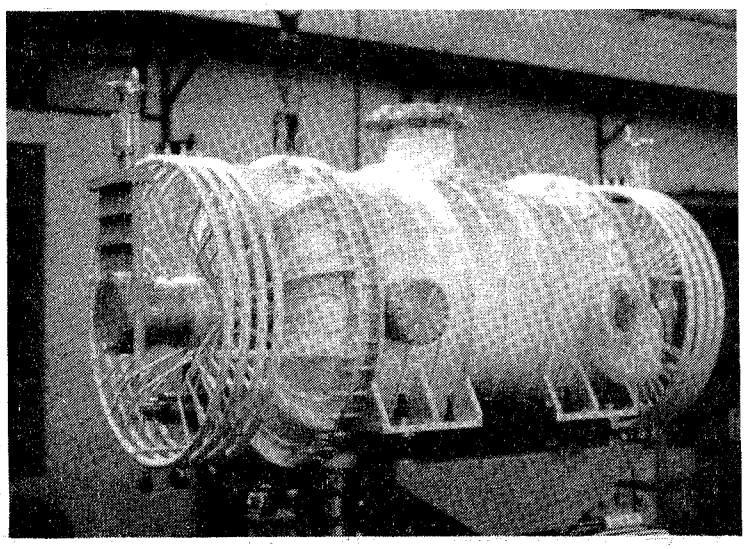

FIG. 9 - The new cavity resonator before evacuating.

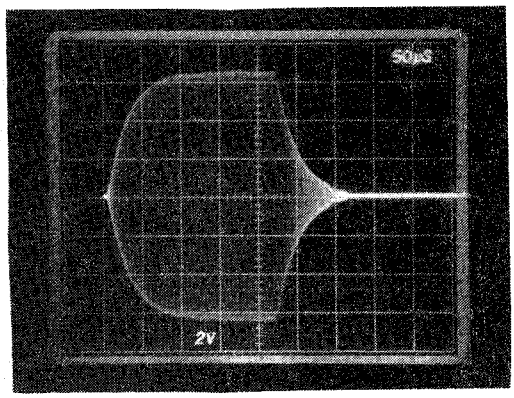

FIG. 10 - RF pulse in the new resonator (v = 40 kV/cm).

This barrier can be however overcome very easily by low power pulsed RF. The simulations of Newtraj code match very well with the experimental results. A resonant trajectory at 12 kV RF gap voltage is presented in Fig.11 but the output data for this simulation show a very low electron multiplication efficiency which is confirmed by the great facility of RF feeding.

This behaviour allows an easy and reliable operation. An RF voltage range from 30 to 250 kV can be obtained. The main parameters are presented in Table II.

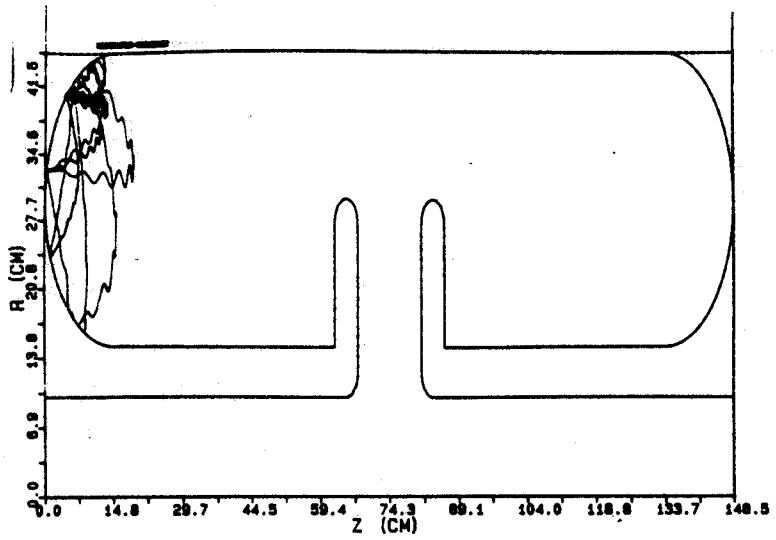

FIG. 11 - Low level resonant trajectoryat 12 kV for the new cavity.

Table II

Resonant frequency	Fo = 51.410 MHz
Accelerating voltage	Va = 200 kV
Unloaded quality factor	Qo = 12,000
Shunt-impedance	Zsh = 2.3 Mohm
Dissipated power	Pd = 18 kW

Conclusions

Experiments performed in our laboratory on various re-entrant resonators have confirmed the usefulness of codes that compute electron trajectories in localizing m.p. discharges. With the aid of such a code we have designed a re-entrant resonator whose shape guarantees freedom from one-point resonant discharges even in the presence of high secondary emission from the surface.

This has been obtained by giving a rounded shape to the end-plates, where such discharges are most probable. Experimental results are fully satisfactory.

Acknowledgements

The authors are grateful to the people of RF and mechanical groups of Adone staff for the support given in the design and test of cavities.

APPENDIX A

The Newtraj code

The Newtraj code uses the RF fields of a monopolar TM mode, as computed by OSCAR-2D simulation code[5], to follow the motion of the electrons inside any reasonable shape of axially symmetric accelerating cavity or structure.

Since the problem to be solved has a rotational symmetry around an axis, we restricted ourselves to compute the motion of the electrons in a plane through that axis.

This choice comes out from the following arguments:

a) the electric field in the cavity lies in the symmetry plane, and the electrons field-emitted from the surface move along the field lines;

b) secondary electrons reemitted by the surface could in principle have the starting velocity not lying in the symmetry plane, but the value of the starting velocity is low (the typical energy is few eV), so the motion in the ϕ direction can be neglected without a significant change in the results;

c) the reemission direction of the backscattered electrons lies in the symmetry plane if the direction of the primary electron does and, for the aforementioned arguments, the velocity of the primary electron can be considered lying in the symmetry plane.

The relativistic equation, in vector form, for an electron moving in the RF field of a resonator is :

$$\dot{\vec{v}} = \frac{e}{m_0\gamma}\left(\vec{E} + \vec{v} \times \vec{B} - \frac{\vec{E}\cdot\vec{v}}{c^2}\vec{v}\right)$$

where $\mathbf{m_0}$ is the electron rest mass, $\mathbf{e}$ is the electron charge, $\vec{\mathbf{E}}$ and $\vec{\mathbf{B}}$ the electric and magnetic fields.

With our assumption of TM monopolar modes and electron motion in the r,z plane, we obtain:

$$\dot{r} = v_r$$

$$\dot{z} = v_z$$

$$\dot{v}_r = \frac{e}{m_0\gamma}\left(E_r - v_z B_\varphi - \frac{\vec{E}\cdot\vec{v}}{c^2}v_r\right)$$

$$\dot{v}_z = \frac{e}{m_0\gamma}\left(E_z - v_r B_\varphi - \frac{\vec{E}\cdot\vec{v}}{c^2}v_z\right)$$

This set of differential equations is easily integrated by a step by step Euler method.

The trajectory is followed until the electron strikes the metallic wall. At the impact point a

secondary electron is generated. The energy and the direction of the new electron are randomly generated accordingly to the distribution of the secondary emission of the cavity wall and the backscattering process.

At each impact the electron yield is stored; the tracking of the electron trajectories is stopped when :

a) the electron leaves the cavity via any coupling hole;
b) the product "impact energy by yield" is lower than a fixed value;
c) the number of RF cycles is higher than a value given as an input datum;
d) the RF phase-lag between two impacts is less than 10°.

Secondary emission model

When an electron, accelerated by the RF field of the structure strikes the cavity wall a new electron is generated by a random process taking into account the probability, related to the value of the impact energy, of producing true secondaries or backscattered.
First, we assume the secondary yield distribution δ as a function of the impact energy U_{im}

$$\delta = \frac{2\,\delta_o\,(U_{im}/U_{max})^{1.2}}{(1+(U_{im}/U_{max})^2)\cdot|\cos\theta|}$$

where :

U_{max} = energy where the maximum of secondary yield is reached (preset in input);
δ_o = maximum value of the secondary yield distribution (preset in input);
θ = impact angle of the electron.

The backscattered yield is: $\eta = \eta_o + (1 - \eta_o)\cdot|\sin\theta|$ where θ is again the impact angle of the electrons.

The first term takes into account the true backscattered yield for the material used for building the cavity.

The second term is the contribution to the yield due to the enhanced backscattered impinging the surface at glancing angle.

For the reemission direction, trues backscattered and secondaries are treated in the same way. In both cases the reemission direction is randomly generated with a "cos θ" distribution around the normal direction to the surface at the impact point. The enhanced backscattered are specularly reflected at the impact point.

The energy of the emitted electrons depends on the reemission process in the following way:

a) for the true secondaries, for an impact energy $U_{im} > U_{max} / 10$ the energy of the reemitted electron is a value preset in input (typically 2-4 eV); for $U_{im} < U_{max} / 10$ the energy of the

secondaries is randomly distributed in the range 0 - U_{im};

b) for the enhanced backscattered the reemission energy is fixed to a value of 0.8 U_{im};

c) for the true backscattered the reemission energy is randomly distributed with the distribution:

$$U_{out} = y\, U_{im} \qquad 0 \le y \le 1$$

$$f(y) = \frac{5+2 \log_{10} (U_{im}/U_{max}) - 2y}{1+ ((5/2) \log_{10} (U_{im}/U_{max}) - y)^2}$$

References

1) J. Halbritter, Particle Accelerator 1972, vol. 3, pp. 163-174.
2) J.P.Budliger et A.Laisne, N.I.M., vol. 61, 1968, pp.253-259.
3) H.Padamsee, IEEE Trans. on N.S., vol. NS-24, 3, June 1977.
4) R.Boni, V.Chimenti, S.Fortebracci, F.Tazzioli, G.Turchetti, IEEE Trans on N.S., vol NS-30, 4, Aug. 1983.
5) P.Fernandes et R.Parodi, 1986 Linac Conf. Proc., pp. 330-332.
6) P.Fernandes et R.Parodi, 1987 Part. Acc. Confer., March 87, Washington.
7) V.Lagomarsino, G.Manuzio, R.Parodi, R.Vaccarone, IEEE Trans. MAG-15 (1979), 25.
8) U.Klein et D.Proch, Gesamtochschule Wupperthal, WU B 78-31 (1978)
9) R.Boni, V.Chimenti, P.Fernandes, R.Parodi, B.Spataro,F.Tazzioli; IEEE, Trans. on N.S., vol.NS-32,5, Oct.1985.